Ecology, 91(6), 2010, pp. 1748–1762

Internally driven alternation of functional traits in a multispecies predator–prey system

Katrin Tirok[1] and Ursula Gaedke

University of Potsdam, Institute of Biochemistry and Biology, Am Neuen Palais 10, 14469 Potsdam, Germany

Abstract. The individual functional traits of different species play a key role for ecosystem function in aquatic and terrestrial systems. We modeled a multispecies predator–prey system with functionally different predator and prey species based on observations of the community dynamics of ciliates and their algal prey in Lake Constance. The model accounted for differences in predator feeding preferences and prey susceptibility to predation, and for the respective trade-offs. A low food demand of the predator was connected to a high food selectivity, and a high growth rate of the prey was connected to a high vulnerability to grazing. The data and the model did not show standard uniform predator–prey cycles, but revealed both complex dynamics and a coexistence of predator and prey at high biomass levels. These dynamics resulted from internally driven alternations in species densities and involved compensatory dynamics between functionally different species. Functional diversity allowed for ongoing adaptation of the predator and prey communities to changing environmental conditions such as food composition and grazing pressure. The trade-offs determined whether compensatory or synchronous dynamics occurred which influence the variability at the community level. Compensatory dynamics were promoted by a joint carrying capacity linking the different prey species which is particularly relevant at high prey biomasses, i.e., when grazers are less efficient. In contrast, synchronization was enhanced by the coupling of the different predator and prey species via common feeding links, e.g., by a high grazing pressure of a nonselective predator. The communities had to be functionally diverse in terms of their trade-offs and their traits to yield compensatory dynamics. Rather similar predator species tended to cycle synchronously, whereas profoundly different species did not coexist. Compensatory dynamics at the community level thus required intermediately strong trade-offs for functional traits in both predators and their prey.

Key words: adaptability; compensatory dynamics; ecosystem function; food web model; functional diversity; functional traits; stability; trade-offs; variability.

Introduction

Classical predator–prey models like the Lotka-Volterra model (Lotka 1925, Volterra 1926) with linear, or the Rosenzweig-McArthur model with nonlinear growth and grazing functions (Rosenzweig and MacArthur 1963) predict predator–prey cycles, or a stable equilibrium with either low predator biomass and the very abundant prey close to its carrying capacity, or the prey suppressed by highly abundant predators. Strong interactions were found in both natural and experimental systems (e.g., Elton and Nicholson 1942, Luckinbill 1979, McCauley et al. 1999, Fussmann et al. 2000). In the field, a pronounced predator–prey cycle is observed in meso- to eutrophic lakes, where the spring algal bloom is typically strongly grazed by large herbivorous zooplankton, such as daphnids, causing a so called clear-water phase (Sommer et al. 1986). However, a remarkably smaller temporal variability across many generations of predator and prey is observed in some diverse plankton communities of, for instance ciliates and algae (Tirok and Gaedke 2007) or rotifers and algae (Yoshida et al. 2007).

Temporal variability of populations and communities is known to depend on diversity (McCann 2000, Hooper et al. 2005, Thebault and Loreau 2005), which itself is influenced by variability. Variable population densities often sum up to produce a relatively constant biomass at the community level, due to simple statistical averaging of independently fluctuating populations (portfolio effect), and/or the higher probability of differential responses to altered environmental conditions (compensatory dynamics; McCann 2000, Hooper et al. 2005, Thebault and Loreau 2006). We focus on how this may arise from different functional traits within communities, whose key role for ecosystem functioning has been increasingly recognized in both aquatic and terrestrial systems (Weithoff 2003, Norberg 2004, McGill et al. 2006).

Manuscript received 15 June 2009; revised 22 September 2009; accepted 1 October 2009. Corresponding Editor: K. D. Winemiller.

[1] Present address: Max-Planck-Institute of Molecular Plant Physiology, Systems Biology and Mathematical Modeling, Am Mühlenberg 1, 14476 Potsdam-Golm, Germany. E-mail: katrintirok@googlemail.com

All organisms face certain constraints in their use of energy and other resources. Obviously resources used for one process, can not be used for another one. This results in well-established trade-offs in the performance of ecological characteristics, such as different feeding and life history strategies (Tilman et al. 1982, Stearns 1992, Huisman et al. 2001, Norberg 2004, Litchman and Klausmeier 2008). Examples include trade-offs between the maximum resource uptake rate and the resource concentration required to achieve half saturation of resource uptake which were observed for different groups, such as phytoplankton (Litchman et al. 2007) and zooplankton (Sommer et al. 2003). For example, raptorial copepods with their low half-saturation constants are more important in oligotrophic, algal-poor systems in contrast to more strongly filtering cladocerans such as daphnids, which are competitively superior in eutrophic, algal-rich waters (e.g., Rothhaupt 1990). Similarly, a high maximum growth rate is often achieved at the cost of a high susceptibility to predation (Grime 1977, Wirtz and Eckhardt 1996, Yoshida et al. 2004, Litchman and Klausmeier 2008). Such rapid growth would be reduced by investment into defense mechanisms, and/or predator avoidance strategies.

In this study, we address the question how two ubiquitous and important features of ecological systems, functional diversity and ecological trade-offs in particular, may influence the dynamics of predator–prey systems, using a mathematical model. The study is inspired by field observations from a large deep lake (Lake Constance). Here, a species-rich community of small fast-growing predators (algivorous ciliates) and their prey (small edible algal species) coexisted with both trophic levels at a high biomass level for numerous generations during the spring bloom under less variable environmental conditions (Müller et al. 1991, Gaedke et al. 2002, Tirok and Gaedke 2007). This means that we did not observe typical predator–prey cycles as would be predicted by simple one-predator–one-prey models. Rather, we observed three remarkable patterns: (1) a high biomass of ciliates and algae relative to their carrying capacity, (2) a lower biomass variability at the community than at the population level, and (3) a lower rate of change in the mean functional traits of the predator and prey communities than in species composition. The data and our model analysis suggest that these patterns were driven by alternations in the contribution of numerous ciliate and phytoplankton species to community biomass resulting from compensatory dynamics. These predator and prey communities comprise functionally different species (e.g., selective and nonselective predators, fast- and slow-growing prey species; Müller et al. 1991, Tirok and Gaedke 2007).

We developed a multispecies model comprising three functionally different predator and prey species. It accounted for differences in feeding preferences and susceptibility to predation, and for the respective trade-offs, i.e., a high growth rate of the prey was connected to a high grazing vulnerability, and a low food demand of the predator was connected to a high food-selectivity and thus to a lower food quantity available for consumption. Our model analysis, which is firmly linked to field observations, provides mechanistic insight into how patterns in population dynamics and compensatory dynamics at the community level may arise from an internal feedback system, originating from the presence of functionally different species and trade-offs that continuously modify the community's properties. Moreover, we show how functional differences can yield either compensatory or synchronous dynamics occurring as intrinsic properties of the system, i.e., independent of external forces, which may vary in time.

Methods

Field data

The model food web is quite general, but it was inspired by field observations from large, deep, mesotrophic Lake Constance, situated north of the European Alps. A detailed description of the study site and of data sampling is provided by Müller (1989), Weisse and Müller (1998), Gaedke et al. (2002), and Tirok and Gaedke (2007). The phytoplankton spring bloom in Lake Constance is dominated by the cryptomonads *Rhodomonas* spp. and *Cryptomonas* spp., and the small centric diatom *Stephanodiscus parvus* (Kümmerlin 1991, Sommer et al. 1993). The latter maintains a hard silicate frustule, which reduces its food quality for ciliates (Skogstad et al. 1993, Müller and Schlegel 1999). Ciliates comprise different feeding modes, and numerous species are known to feed selectively on small phytoplankton (Fenchel 1987, Verity 1991, Hamels et al. 2004). Interception feeders capture and process single prey particles and are thus supposed to be highly selective, whereas filter feeders strain suspended food particles from surrounding water and thus feed less selectively (Fenchel 1987). Lake Constance data indicated that ciliated filter feeders benefit from a high quantity of mixed food algae, including small diatoms, whereas interception feeders depend on high-quality cryptomonads, which are sometimes less abundant (Müller and Schlegel 1999, Tirok and Gaedke 2007). These two feeding types may represent two different strategies to meet the trade-off between food quantity and quality. A trade-off is also established in the small phytoplankton community, where low quality diatoms demand silicate, and may suffer from losses by sedimentation. Furthermore, diatoms are non-motile in contrast to cryptomonads. Motility increases the resource availability and thus growth rate, but also the likelihood of predator encounter and thus grazing susceptibility (Reynolds 1997).

Calculations of field data were done with the most abundant five small edible algal and nine ciliate species, which contribute together 84% and 88% to the total

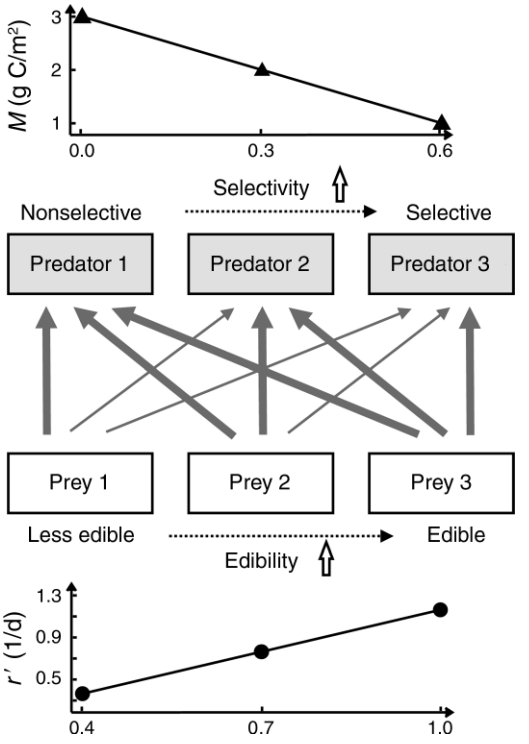

FIG. 1. Feeding relationships and trade-offs in the growth and grazing characteristics of the predator (top) and the prey community (bottom) in the multispecies model. The direction of arrows corresponds to "is eaten by," and their thickness to the interaction strength, i.e., the different feeding preferences of the predator species (q_{ij}). The value of the half-saturation constant M (Eq. 10) and the potential growth rate r' (Eq. 9) are linearly related to the food selectivity of the predator and to the edibility of the prey, respectively.

biomass, respectively (compare Table 1 in Tirok and Gaedke 2007). To compare model results with the field data, we calculated the weighted mean population CV (coefficient of variation; see *Quantifying variability and diversity*, Eq. 16), the community CV (Eq. 17), and the damping (Eq. 19) from the field data.

Multispecies model

We extended a classical one-predator–one-prey model based on the equations of Rosenzweig and MacArthur (1963) by adding two more predator and prey species which resulted in a multispecies model with six state variables and nine feeding interactions (Fig. 1). Prey (A_i) and predator (C_j) dynamics ($i, j = 1, \ldots, 3$) are described by

$$\frac{dA_i}{dt} = r_i A_i - \sum_j g_{ij} C_j \tag{1}$$

$$\frac{dC_j}{dt} = \left(e \sum_i g_{ij} - d \right) C_j \tag{2}$$

$$r_i = r_i' \left(1 - \frac{\sum_k A_k}{K} \right) \tag{3}$$

$$g_{ij} = g' \frac{q_{ij} A_i f_i}{(\text{food}_j + M_j)} \tag{4}$$

$$\text{food}_j = \sum_i q_{ij} A_i f_i \tag{5}$$

$$f_i = \frac{A_i}{(A_i + A0)} \tag{6}$$

with $A_{i(k)}$ indicating prey species $i(k)$ and C_j indicating predator species j.

Prey growth is logistic with the maximum growth rate r_i' and the carrying capacity K. Predator grazing is similar to a Holling-Type-II functional response with maximum grazing rate g_j', half saturation constant M_j, feeding preferences q_{ij}, total food concentration food_j, and prey density function f_i, which reduces grazing at very low prey densities. Growth efficiency and mortality rate are represented by e and d, respectively. Values and a description of parameters are given in Table 1.

The prey species differ in their maximum growth rates and compete according to a common carrying capacity (cf. Eq. 3, Table 1), but have the same critical prey density $A0$ (cf. Eq. 6, Table 1). They suffer losses by grazing of the predators in dependence of their edibility (edib_i, Eq. 7), which is calculated from the feeding preferences q_{ij}, as is the food selectivity of the predators (sel_j, Eq. 8):

$$\text{edib}_i = \frac{1}{3} \sum_j q_{ij} \tag{7}$$

$$\text{sel}_j = \frac{1}{3} \sum_i (1 - q_{ij}). \tag{8}$$

The feeding preference q_{ij} specifies the proportion of prey A_i, which can be ingested by predator C_j. A highly selective predator can ingest nearly all of its preferred prey ($q \approx 1$), but only a small proportion of other prey species ($q \ll 1$). The effective composition of the food of a predator, food_j, depends on the actual abundances of the individual prey species in addition to the feeding preferences (Eq. 5). That is, if all prey species are equally abundant, the diet of the predator contains a high percentage of the preferred prey (high q). If the preferred prey is rare compared to other prey species, the latter may dominate in the food of the predator, and the prey concentration that is available as food is lower.

The feeding preferences q define the structure of the model food web as they influence the number and the relative importance of feeding links (Fig. 1, Table 1). We defined predator 1 (C_1) as a nonselective consumer, feeding on all prey species equally well. In contrast, predator 3 (C_3) is highly selective, and feeds mainly on

TABLE 1. Description and values of parameters for the multispecies model with $i, j = 1/2/3$.

Name	Description	Unit	Value
r_i	maximum prey growth rate†	1/d	0.37/0.77/1.17
K	carrying capacity	g C/m^2	8
g'	maximum grazing rate	1/d	1.7
M_j	half-saturation constant‡	g C/m^2	3/2/1
e	growth efficiency		0.2
d	mortality rate	1/d	0.15
$A0$	critical prey density	g C/m^2	0.02
q_{i1}	feeding preference of predator C_1 on prey A_i		1/1/1
q_{i2}	feeding preference of predator C_2 on prey A_i		0.1/1/1
q_{i3}	feeding preference of predator C_3 on prey A_i		0.1/0.1/1
edib$_i$	edibility of prey species§		0.4/0.7/1
sel$_i$	food selectivity of predator species¶		0/0.3/0.6

† Derived from Eq. 9 with $m_{r'} = 1.33$ and $b_{r'} = -0.16$.
‡ Derived from Eq. 10 with $m_M = -3.33$ and $b_M = 3.0$.
§ Derived from Eq. 7.
¶ Derived from Eq. 8.

prey 3 (A_3), and less on prey 1 (A_1) and 2 (A_2). Predator 2 (C_2), in between, feeds well on A_2 and A_3, and less on A_1. These differences result in the highest available food quantity for the nonselective consumer C_1, and the lowest available food quantity for the selective consumer C_3 (compare Eq. 5). We defined such a gradient also for the prey community, in which A_1 is a less-edible prey species only efficiently grazed by C_1. In contrast, A_3 represents a highly edible species equally eaten by all predators. A_2, in between, is well eaten by C_1 and C_2, and less by C_3. Consequently, the highly edible species A_3 suffers from higher grazing losses compared to A_2 and A_1, in particular. For simplicity we chose a symmetric food web, with the feeding preference either 1 (preferred prey) or 0.1 (non-preferred prey). This resulted in "equal" distances of the edibility between the prey species and of the food-selectivity between the predator species.

The term describing the grazing of different prey species (g_{ij}, Eq. 4) was adopted from Baretta-Bekker et al. (1995, 1998). The prey density function f only modifies the grazing rate at very low prey abundances close to the critical prey density $A0$, around which the curve becomes sigmoidal. For very low values of $A0$, as used here, the function is closer to a Holling-Type-II than a Holling-type-III functional response. Introducing f and $A0$ keeps the model dynamics in a realistic time span, but does not change the overall outcome of the model. Competitive exclusion in the model is not prevented by this term.

Parameter values for the different species were systematically chosen to represent ecological trade-offs as anticipated for the natural communities of algae and ciliates (Wirtz and Eckhardt 1996, Reynolds 1997, Norberg 2004). In the model, the three prey species differ in their growth characteristics (maximum growth rate r'), and the three predator species differ in their feeding characteristics, that is, in their preferences for the different prey species (q), and in the food quantity they require to achieve half maximum grazing rates (M).

The highly edible prey species A_3 has the highest potential growth rate. That is, it can exploit its resources very fast compared to the slower growing species A_2 and A_1, in particular (Fig. 1). The most selective predator C_3, i.e., the one with a strong feeding preference for only one prey species, has the lowest half-saturation constant. This means, it competes successfully at low to medium prey abundances, when its preferred prey dominates the total prey community. The nonselective predator C_1 has a high half-saturation constant. It competes successfully at high abundances of a mixed prey community. For simplicity, we chose linear relationships for each trade-off (r_i, M_j) with a "cost" parameter (slope m), and a "shape" parameter (intercept b; Fig. 1):

$$r_i' = m_{r'} \times \text{edib}_i + b_{r'} \tag{9}$$

$$M_j = m_M \times \text{sel}_j + b_M. \tag{10}$$

Parameters of the trade-off functions (slope and intercept) were chosen to get realistic values, i.e., different, but still within the ecologically reasonable range (Table 1). The carrying capacity of the prey community was estimated from peak biomass values of the edible algal community in Lake Constance during the spring bloom (approximately 4–8 g C/m^2; Müller 1989, Weisse and Müller 1998, Gaedke et al. 2002, Tirok and Gaedke 2007). In a sensitivity analysis, we systematically tested other values of the model parameters (see *Sensitivity analysis*). Initial biomass values were chosen in the range of observed values in Lake Constance during the spring bloom, i.e., $\sum_i A_i = 2$–4 g C/m^2 and $\sum_j C_j = 0.5$–1.5 g C/m^2.

For summarizing the properties of the predator and prey communities, weighted mean values of selected attributes were calculated.

Mean edibility for the prey community was calculated as

$$\text{edib} = \frac{\sum_i (A_i \times \text{edib}_i)}{\sum_i A_i} \tag{11}$$

and mean maximum growth rate was calculated as

$$r' = \frac{\sum_i (r_i' \times A_i)}{\sum_i A_i}. \quad (12)$$

Mean food selectivity for the predator community was calculated as

$$\text{sel} = \frac{\sum_j (C_j \times \text{sel}_j)}{\sum_j C_j} \quad (13)$$

and mean half-saturation constant was calculated as

$$M = \frac{\sum_j (M_j \times C_j)}{\sum_j C_j}. \quad (14)$$

Sensitivity analysis

To test the robustness of the model behavior we ran the model with systematically changed parameter values, and different initial values. First, we altered the parameter values of the equations for r_i' and M_j by maintaining the trade-offs, but changing their extent, i.e., their slopes ($m_{r'}$, m_M, Eqs. 9 and 10). Slopes of zero correspond to same growth rates for the prey species and same half-saturation constants for the predator species, but still different edibilities and food selectivities. Steeper slopes imply more pronounced changes of r_i' with edibility, and of M_j with food selectivity. Along with the slopes, we altered the intercepts of the equations in such a way that the parameter values of species A_2 and C_2 were retained. That is, changing the "cost" parameters $m_{r'}$ and m_M involved changes of the other trade-off parameters, $b_{r'}$ and b_M. We altered $m_{r'}$ between 0 and 2.23 (0.03 to 2.23 in steps of 0.05, $b_{r'} = -0.7m_{r'} + 0.77$), and m_M between 0 and −5.03 (−0.03 to −5.03 in steps of 0.1, $b_M = -0.3m_M + 2$).

To analyze the influence of the trade-off parameters on the prey and predator community in terms of composition, damping, and synchronous vs. compensatory dynamics, we calculated the evenness, i.e., standardized diversity (Eq. 18) within the prey and predator community, the damping of biomass variability from the population to the community level (Eq. 19), and the variance ratio (Eq. 20). An evenness ≥ 0.7 implies coexistence of all species with the mean relative importance of the individual species within $0.02 < \bar{p}_k < 0.75$. An evenness lower than 0.5 typically reflects predominance of one species ($\bar{p}_k \gtrsim 0.85$). Extinction of one species can occur from an evenness of 0.63 and lower. The variance ratio is a measure of synchronization vs. compensation in the communities (cf. *Quantifying variability and diversity*). The variance ratio was only calculated for parameter combinations yielding an evenness ≥ 0.5.

Second, we altered the values of the feeding preferences defining the structure of the model food web. In the standard run, we chose a symmetric food web where the predator either strongly prefers a prey species ($q = 1$) or does not prefer it ($q = 0.1$). This resulted in "equal" distances of the edibility between the prey species and of the food-selectivity between the predator species. To break up this symmetry, we made two species more similar to each other compared to the third one by changing the q values. For example, decreasing $q_{22} \ll 1$ (feeding preference of C_2 for A_2) decreased the functional differences between A_2 and A_1, and between C_2 and C_3, and increased those between A_2 and A_3, and between C_2 and C_1 at the same time.

Third, we altered the values of the intercepts of the trade-off functions individually (Eqs. 9 and 10), which define the absolute values of the maximum prey growth rate and the half-saturation constant. We also changed the carrying capacity (K) of the prey, and the maximum grazing rate (g'), growth efficiency (e), or mortality rate (d) to consider the maximum gross growth rate of the predator. The absolute values of the growth and grazing rates are known to influence the dynamic behavior of the classical one-predator–one-prey models (Lotka 1925, Volterra 1926, Rosenzweig and MacArthur 1963).

Fourth, we started the simulations with different initial values to test for alternative attractors. We also tested the potential impact of the initial biomass distribution across species by using either a uniform or a skewed distribution.

Quantifying variability and diversity

The temporal variability of predator and prey biomass was assessed with the coefficient of variation (CV),

$$\text{CV} = \frac{s}{\bar{x}}$$

with s = standard deviation and $\bar{x}$ = mean value.

Population CV was calculated as

$$\text{CV}_k = \frac{s(X_k)}{\bar{X}_k} \quad (15)$$

with $k = i, j$ and $X = A, C$.

Weighted mean population CV was calculated as

$$\text{CV}_{\text{pop}} = \frac{\sum_k (\text{CV}_k \times \bar{X}_k)}{\sum_k \bar{X}_k}. \quad (16)$$

Community CV was calculated as

$$\text{CV}_{\text{comm}} = \frac{s\left(\sum_k X_k\right)}{\sum_k \bar{X}_k}. \quad (17)$$

Diversity was estimated with the Shannon-Wiener index and standardized for the species number, which gives the evenness. It was calculated from the mean relative importance of the three prey or predator species

$$J = \frac{-\sum_k (\bar{p}_k \times \log_{10} \bar{p}_k)}{\log_{10} S} \quad (18)$$

with $k = i, j$, $\bar{p}_k$ = mean relative importance of species k and S = number of species.

Damping of the temporal variance from the population to the community level within the predator and prey community was calculated as

$$\text{Damping} = \frac{\text{CV}_{\text{pop}}}{\text{CV}_{\text{comm}}}. \quad (19)$$

The variance ratio (V) is the ratio of the community variance (derived from the variances and covariances of the populations) to the sum of the population variances. The variance ratio is equal to 1 when the sum of population covariances is zero (population dynamics are independent), whereas values greater (less) than 1 indicate positive (negative) covariances and thus synchronous (compensatory) dynamics among populations (Schluter 1984, Vinebrooke et al. 2003). Values of $V \approx 1$ may also arise when synchronous and compensatory dynamics alternate during the time span considered:

$$V = \frac{s^2\left(\sum_k X_k\right)}{\sum_k s^2(X_k)} = \frac{\sum_k s^2(X_k) + 2\sum_k \sum_l \text{cov}(X_k, X_l)}{\sum_k s^2(X_k)} \quad (20)$$

with s^2 = variance, $k = i, j$, $l = i, j$, $l \neq k$ and $X = A, C$.

Data representation

Calculations were done in MATLAB 7.x R2007b (The MathWorks, Munich, Germany) and SAS version 9 (SAS Institute 2002). All model simulations were run over 10 000 time steps to get away from transient oscillations. Graphics and further calculations, including the CV and damping, were done for the last 400 time steps (9600–10 000 days). We consider equilibrium conditions as the spring bloom in Lake Constance represents a period where internal processes are dominating. During the spring bloom, the variability of total algal and ciliate biomass is low compared to that over the course of the season. Field data are shown for late winter and spring, February until mid-June (values/m^2 correspond to 20 m^3). CV and damping were calculated for the spring bloom, mid-March until end of May (day of the year = 74–151, 78 d) in 1991 and 1996, two years with a long-lasting spring bloom in Lake Constance.

Results

Internally driven alternation of functional traits

The multispecies model revealed coexistence of the three predator and the three prey species across a range of parameter values and critical conditions. Within the simulation period of 10 000 time steps, the system showed complex periodic cycles of predator and prey biomass, i.e., a closed curve (limit cycle), when using the standard parameter set inspired by the field data (Table 1). The typical uniform predator–prey cycles with quarter-period phase lags as known from one-predator–one-prey models were not preserved in the multispecies model. The different species exhibited more or less pronounced oscillations, whereas total predator and prey biomass, $\sum_j C_j$ and $\sum_i A_i$, oscillated moderately at high biomass levels ($\approx$ 1–2 g C/m^2 and $\approx$ 0.7–4 g C/m^2 for predators and prey, respectively), and rather close to the prey capacity (Fig. 2a, b)

The relative contribution of individual species to total community biomass varied in time, and neither a predator nor a prey species reached a lasting predominance (Fig. 2c, d). The properties of the prey and the predator community, as indicated by the mean edibility and potential growth rate of the prey, and the mean food selectivity and half-saturation constant of the predator, varied systematically over time, driven by alternations in the different prey and predator species (Fig. 2e, f; for calculations, see *Methods: Quantifying mean properties of the predator and prey community*). Thereby, the rate of change of the community properties was lower than that of the species composition. We thus observed an internally driven alternation of functional traits that resulted in compensatory dynamics at the community level. This was not the only possible outcome, as the populations could also cycle in synchrony when using other parameter values, in which case, the stabilization of total plant and herbivore biomass would be reduced.

The explicit depiction of functionally different species in the model enables us to unravel the underlying mechanisms (Fig. 2). For example, the prey community was characterized by a high edibility when A_3 dominated, and the predator community was less selective when C_1, the nonselective consumer, dominated. A high edibility of the prey community promoted the selective consumer C_3, which then exerted a high and selective grazing pressure on the highly edible prey (i in Fig. 2e; Fig. 2a–d). Subsequently, the proportion of highly edible prey decreased, and less edible species were released from competition and increased in density (Fig. 2a–d), which resulted in a low edibility of the prey community (ii in Fig. 2e). This in turn promoted the consumer C_1, which is less selective (iii in Fig. 2e; Fig. 2a–d). Hence, A_1 was reduced and the highly edible prey A_3 gained in importance again (iv in Fig. 2e; Fig. 2a–d). These species alternations represent an ongoing cyclic change in relative species densities without any indica-

tion of fading out within 10^7 time steps. Species biomasses always came back to the complex limit cycle. C_1 and C_2 each increased with A_1 and A_2, respectively, and benefitted also from the following peak of A_3 before breaking down due to food shortage (Fig. 2a–d) That is, C_1 and C_2 reached longer peak durations than the respective prey species. The selective grazer C_3 only gained in importance when its preferred prey A_3 reached high biomasses, and hardly dominated in the predator community with the present parameterization. The fast-growing species A_3 and C_3 oscillated with a higher frequency than the slower-growing species (Fig. 2a–d).

The variability of biomasses, indicated by the coefficient of variation, was higher at the species level than at the community level in both, the field data and the multispecies model (Table 2). The weighted mean population CV of the simulated prey populations was rather similar to those of the algal populations in Lake Constance. The variability of the predator populations and that of the prey and predator communities was lower in the model than in the data. Overall, accounting for functionally different predator and prey species dampened the variability of the total predator and prey biomasses (Fig. 2a,b; Table 2).

Sensitivity analysis

Changing the standard parameter set (Table 1) revealed that all six species coexisted over a wide parameter range, and we observed compensatory as well as synchronous dynamics among the different species. If not mentioned otherwise, we obtained for all tested parameter combinations stable limit cycles of different complexity.

Changing functional diversity.—To test the sensitivity of the model behavior to the extent of functional differences among species, we ran the model with systematically changed values of the trade-off parameters ($m_{r'}$, m_M, $b_{r'}$ and b_M; for details, see *Methods: Sensitivity analysis*). The three prey and predator species coexisted over a broad parameter space indicated by the high evenness (Fig. 3a). The evenness of the prey community was less sensitive to the steepness of the trade-off functions and thus to the extent of functional diversity in both the prey and the predator community. A low prey evenness was only observed when the predator species were similar (very low absolute values of m_M, far low region in Fig. 3a). In that case, the fast-growing, highly edible, prey species A_3 was favored by increasing differences in the prey growth rates. That is, with increasing $m_{r'}$ the growth rate of A_3 increased, whereas that of A_1 decreased, and that of A_2 remained unchanged. The evenness of the predator community depended on functional diversity in the prey community and less on that in the predator community. If the prey species were similar (small values of $m_{r'}$, left region in Fig. 3b, the nonselective grazer C_1 was favored. The more selective predators C_2 and C_3 were favored and increasingly outcompeted C_1 by higher growth rates of their preferred prey species (high values of $m_{r'}$, right-hand region in Fig. 3b) or by their lower half-saturation constants compared to C_1, when the functional differences in the prey or predator community increased.

Within the parameter space yielding a fairly even representation of all predator and prey species, we observed various patterns of synchronization, compensation, and damping. Damping from the species to the community level always required functionally different prey and predator species, in particular (Fig. 3c, d). A high damping was associated with a low variance ratio ($V \ll 1$) indicating compensatory species dynamics (Fig. 3d, e). Synchronization of the prey or the predator species ($V \gg 1$) prevented damping in the prey or the predator community, respectively. A considerable damping combined with a high evenness was observed for a parameter space with intermediate differences between the species ($m_M = -2.93$ to -4.53, $m_{r'} = 0.78$ to 1.98), indicated by the white square in Fig. 3, and represent similar dynamics as observed in Lake Constance, where many species coexisted with similar biomasses during the spring bloom.

To obtain a better understanding of the different patterns in evenness, damping, and variance ratios, we considered four parameter combinations representing either rather similar or very different species in more detail (marked as 0, A, B, and C in Figs. 3 and 4). In parameter combination 0, predator and prey species were simulated without trade-offs ($m_M = 0$, $m_{r'} = 0$), i.e., all prey species had the same growth rates ($r_i = 0.77$) and all predator species the same half-saturation constants ($M_j = 2$). The species only differed in the functional trait values edibility and food selectivity and thus their trophic interactions. In this scenario, the nonselective consumer C_1 outcompeted C_2 and C_3 (low evenness in the predator community) and synchronized the prey species (high variance ratio and high evenness in the prey community) which prevented damping (Figs. 3, 4a). This corresponds to a model with three identical prey species and one predator feeding on all prey species equally. The prey species gained a relatively low biomass compared to their capacity with very low temporal variability due to rather strong top-down control of the nonselective predator with an intermediately high half-saturation constant.

In contrast, in parameter combination A, the three predator and prey species strongly differed from each other ($m_M = -4.83$, $m_{r'} = 2.23$). This parameter combination revealed low damping at the community level, and a low evenness in the predator community due to extinction of consumer C_1. The less-edible prey A_1 obtained only a low biomass, which resulted from its low potential growth rate ($r_1' = 0.10$). Hence, A_1, which is almost exclusively exploited by C_1, did not enlarge the food concentration of C_1 and thus, did not compensate for its high half-saturation constant ($M_1 = 3.5$ compared to $M_2 = 2$, and $M_3 = 0.5$). The other species were temporarily in and temporarily out of phase ($V \approx 0.8$–1.5) which together with the temporal dominance of one species

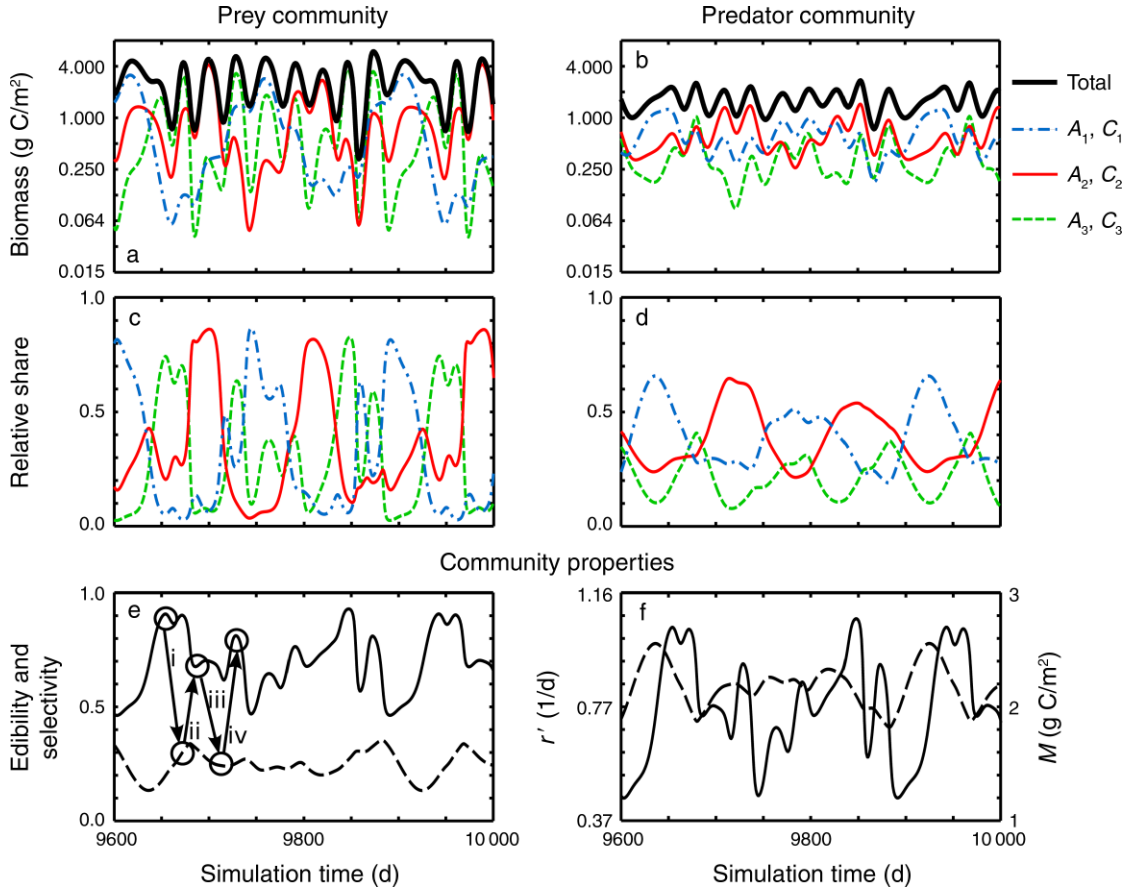

FIG. 2. Simulation results of the multispecies model over 400 time steps. (a, b) Biomass of (a) the prey and (b) the predator (black thick line = total biomass, colored lines = individual species). Note the logarithmic scale of the y-axis. For parameter values, see Table 1. (c, d) Relative share of the individual (c) prey and (d) predator species in community biomass. (e, f) Mean functional traits of (e) the prey community and (f) the predator community. Mean prey edibility (solid line) and predator food selectivity (dashed line) are shown in panel (e), and mean maximum growth rate of the prey (solid line) and mean half-saturation constant of the predator (dashed line) are shown in panel (f). Numbers i–iv in panel (e) depict the transitions between different community properties and are explained in detail in *Results: Internally driven alternation of functional traits*.

(A_2, C_2) resulted in some pronounced peaks and troughs in community biomass and in little damping (Fig. 4b).

In parameter combination B, very different predator, but less different prey species were considered ($m_M = -4.58$, $m_{r'} = 0.53$). This combination resulted in the highest observed damping (≥ 5), despite a rather low evenness in the predator community. The high damping was due to pronounced compensatory dynamics ($V \ll 1$) in the prey community, mainly by A_1 and A_2, which built up a relatively high biomass compared to their

TABLE 2. Coefficient of variance (CV) for populations and communities of the multispecies model and of field data.

	Model		Field data 1991		Field data 1996	
	Prey	Predator	Algae	Ciliates	Algae	Ciliates
CV_1	1.04	0.55				
CV_2	0.89	0.44				
CV_3	1.04	0.43				
CV_{pop}	0.99	0.46	1.19	1.11	0.93	1.19
CV_{comm}	0.48	0.27	0.77	0.66	0.63	0.59
Damping	2.04	1.74	1.54	1.69	1.47	2.02

Notes: CV_1, CV_2, CV_3, are CVs of individual prey species A_i or predator species C_j; CV_{pop} is the mean population CV; CV_{comm} is the CV of the prey or predator community; damping is the damping in the biomass variability from the population to the community level. See *Methods: Quantifying variability and diversity*.

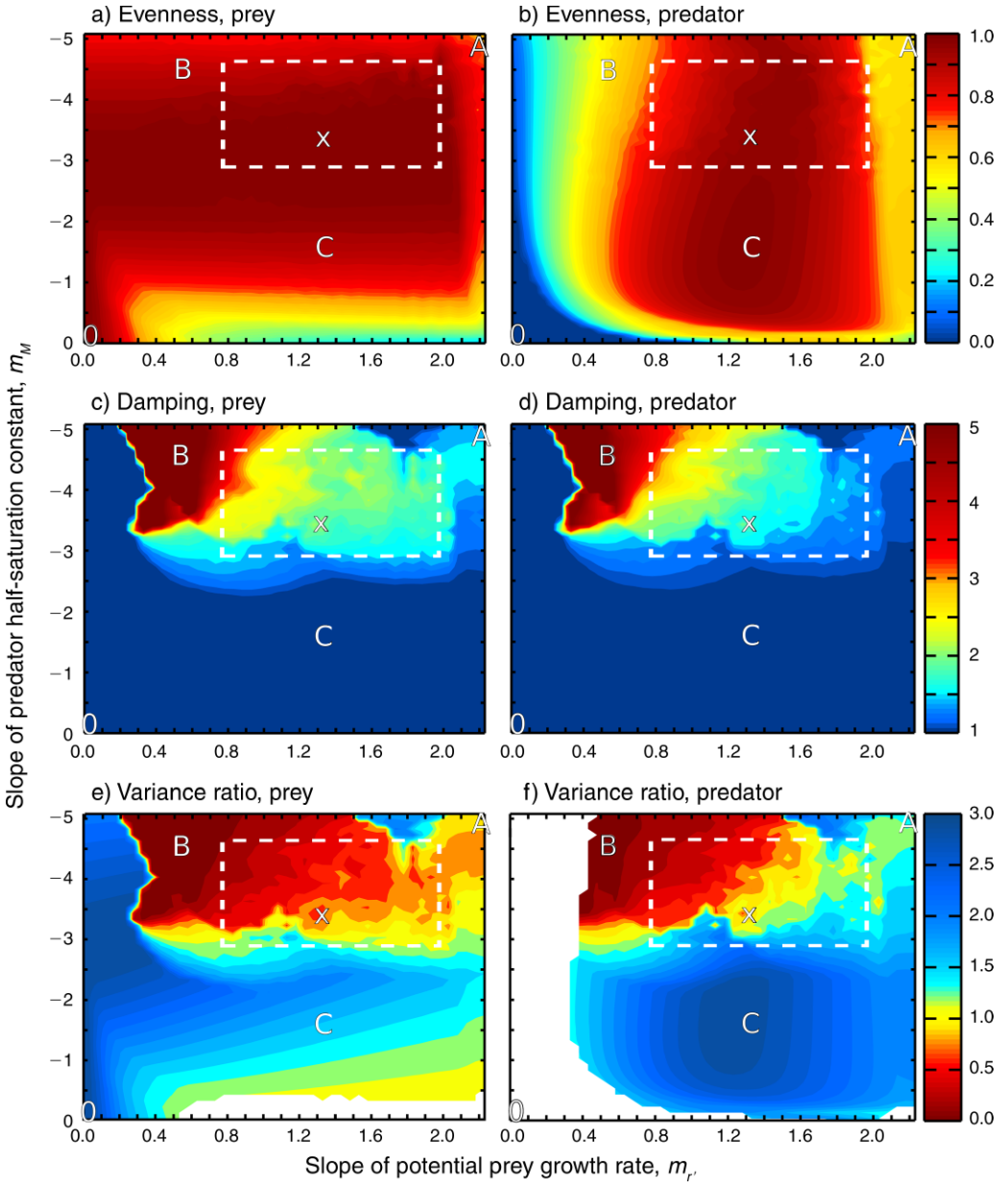

FIG. 3. Influence of the trade-off "cost" parameters $m_{r'}$ (*x*-axis) and m_M (*y*-axis) on (a, b) the evenness, (c, d) the damping of the biomass variability from the population level to the community level, and (e, f) the variance ratio of the prey (a, c, e) and predator (b, d, f) community. The *x*-axis represents the trade-off between maximum growth rate and grazing vulnerability of the prey, and the *y*-axis the trade-off between required and available food quantity of the predators. Increasing cost values imply larger differences between the individual prey or predator species, i.e., a higher functional diversity. The evenness was calculated from the mean relative importance (time = 9600–10 000 d) of the three prey or the three predator species (Eq. 18), the damping from the mean population CV and the community CV (time = 9600–10 000 d; Eq. 19), and the variance ratio from the community variance and the sum of the population variances (time = 9600–10 000 d; Eq. 20). The variance ratio was not calculated for parameter combinations yielding an evenness <0.5 (white areas). Dark blue regions of evenness ($J = 0$) correspond to scenarios where only one species was left and the other two went extinct. X marks the standard parameter combination (Table 1) used in Fig. 2. The dashed white square borders the parameter space where considerable damping was combined with high evenness as it was observed in Lake Constance. 0, A, B, and C mark combinations outside this parameter space, and corresponding time series are shown in Fig. 4 (for details, see *Results: Sensitivity analysis*).

capacity (Fig. 4c). The low evenness resulted from a dominance of the nonselective consumer C_1 ($\bar{p}_1 = 0.82$), which benefited from the relatively high growth rate of the least edible prey species A_1 ($r'_1 = 0.61$) compared to A_3 ($r'_3 = 0.93$). C_1 almost exclusively exploited A_1 which compensated for its high half-saturation constant ($M_1 = 3.4$). The latter prevented in turn a strong top-down control of A_1 and A_2 and thus synchronization.

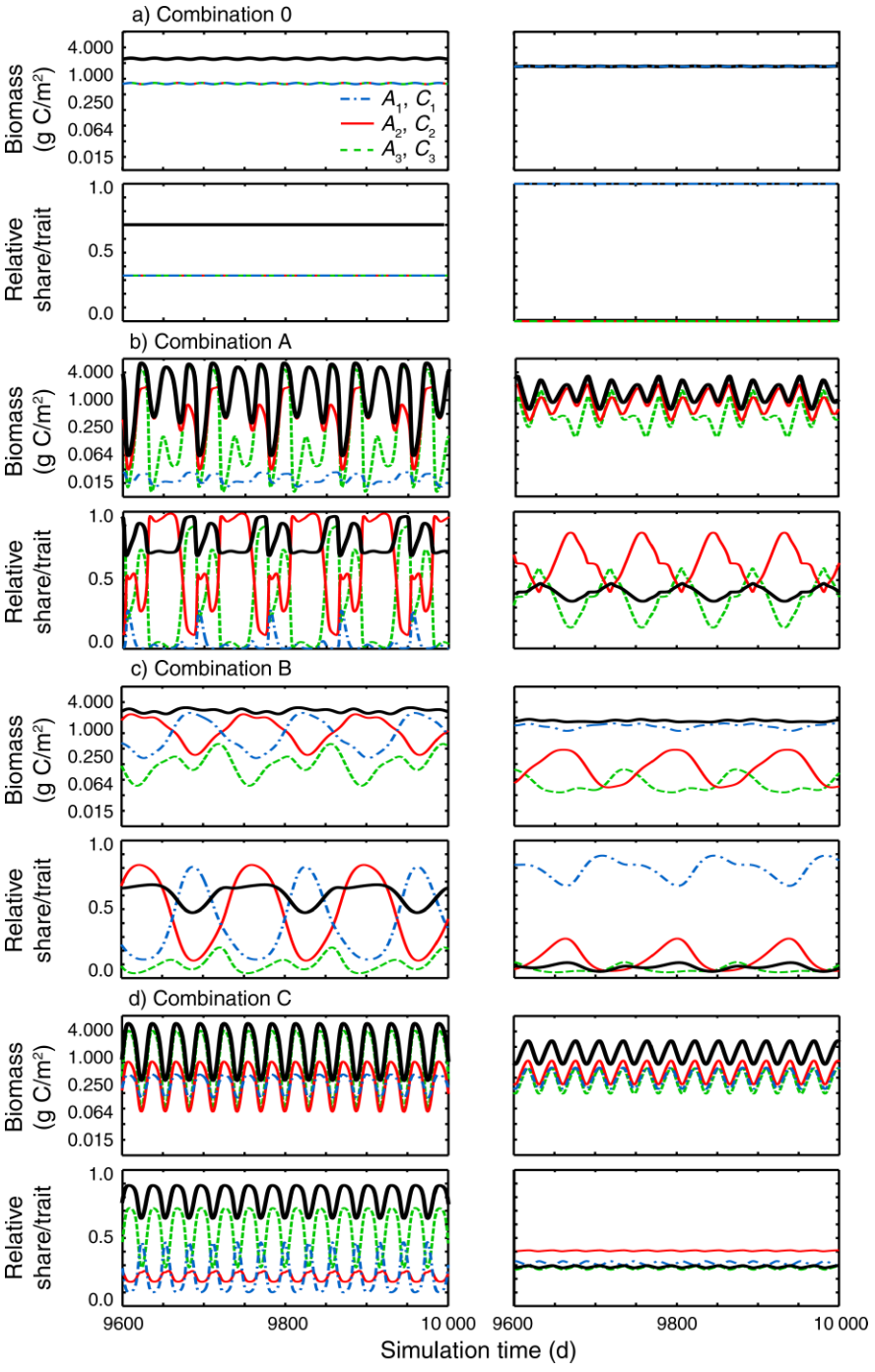

FIG. 4. Simulation results of the multispecies model with altered trade-off parameters according to combination 0, A, B, and C in Fig. 3 and described in *Results: Sensitivity analysis*. (a) Simulations with parameter combination 0, (b) simulations with parameter combination A, (c) simulations with parameter combination B, and (d) simulations with parameter combination C. In all four cases, the upper panels show total biomass (black line) and individual species biomasses (colored lines) of the prey (left) and predator community (right); the lower panels show relative share of the individual species (colored lines) and mean functional traits edibility and food selectivity (black line) in the prey (left) and predator community (right).

In parameter combination C, rather similar predator and intermediately different prey species were simulated ($m_M = -1.58$, $m_{r'} = 1.33$), which resulted in very little damping and a high evenness. The first arose from strong synchronization of all predator and prey species ($V \gg 1$). Synchronization of the predators was promoted by their low differences in the half-saturation constants ($M_1 = 2.5$, $M_2 = 2.0$, $M_3 = 1.5$), and caused

synchronization in the prey community. The high evenness resulted from coexistence of all species, without a predominance of any one species (Fig. 4d).

Breaking up the symmetry of the food web.—In the standard run, the food web was symmetric with "equal" distances of the edibility between the prey species and of the food selectivity between the predator species. This symmetry was not mandatory for the dynamics, i.e., an ongoing change of species composition and a coexistence of predator and prey at high biomass levels. Decreasing the functional differences between two species, e.g., between A_2 and A_1 by decreasing $q_{22} \ll 1$ (e.g., to 0.5) did not change the overall pattern. When two species became very similar they cycled rather synchronously and strongly compensatory to the third one. Making all species more similar by using more similar feeding preferences ($0.1 < q < 1$) eventually resulted in synchronization of all species, irrespective of the symmetry of the food web. Cyclic species displacements and thus compensatory dynamics disappeared under these conditions which could not be balanced by increasing the steepness of the trade-off in the prey community (increasing $m_{r'}$).

Changing absolute parameter values.—Within an ecologically reasonable range, the model behavior was not sensitive to changes in the intercept of the trade-off functions (cf. Eqs. 9 and10), which defines the absolute values of the maximum growth rates (r_i') or half-saturation constants (M_j; cf. Fig. 1). Changing the carrying capacity within $3 \leq K \leq 17$ conserved the cyclic changes in species abundances. Enrichment (increasing K) caused a higher biomass variability and faster cycling of the prey and the predator communities. Changing the absolute value of the maximum grazing rate (g') influenced the dynamic behavior of the model which ranged from extinction of the predator ($g' \leq 1.03$, other parameters as in Table 2) to a complex limit cycle ($1.04 \leq g' \leq 2.30$), and a simple limit cycle ($g' > 2.30$) with all species synchronized. When all predators went extinct ($g' \leq 1.03$), the three prey species coexisted and the initial grazing pressure, i.e., the value of g' in combination with the initial biomasses of the three predator species, determined which prey species reached a predominance. Increasing the growth efficiency e or decreasing the mortality rate d had comparable effects as increasing g' as all three parameters affect the growth rate of the predators. Setting the critical prey density ($A0$) to zero did not change the overall model behavior, i.e., the cyclic changes in species abundances and the associated compensatory dynamics and damping. However, it resulted in stronger grazing on already low prey abundances and thus in cycles with larger amplitudes and lower frequencies of the individual species. This yielded a temporal predominance of individual species.

Changing initial conditions.—The model behavior was not sensitive to changes in initial conditions (total predator and prey biomass and species composition) within a tested range of 0.1–10 g C/m^2 for both, the predator and the prey community in different combinations, and for different values of the maximum grazing rate g'.

Discussion

Comparison of field data and model simulations

Our multispecies model including realistic eco-physiological trade-offs revealed coexistence of numerous species exhibiting an ongoing cyclic pattern of changing species abundance in both the predator and the prey community for a wide parameter range, similar to our field observations. These model dynamics were driven by internal feedback mechanisms. In accordance with our and other field studies (Hooper et al. 2005), the biomass variability of the communities was lower compared to the populations.

The Lake Constance data showed three remarkable patterns in the biomass dynamics during the spring bloom, from mid-March until End of May, when external forcing was of relatively minor importance. (1) Coexistence of predators (algivorous ciliates) and their prey (small algae) at a high biomass level relative to their capacity (Fig. 5a, b); (2) large fluctuations of individual ciliate and algal species, but a relatively constant total biomass of ciliates and small algae (Fig. 5a, b), that is a damping of biomass variability from the population to the community level; (3) a lower rate of change of community-level properties than that of the species composition. The data suggest that these patterns were driven by an alternation of numerical importance of the two predator groups, filter feeders and the more selective interception feeders, as of the two prey groups, the less edible non-cryptomonads, mainly consisting of small centric diatoms, and the highly edible cryptomonads (Fig. 5c, d). All these patterns were also produced by the multispecies predator–prey model (cf. Fig. 2a, b).

Although the model is rather general in the way it includes trade-offs related to feeding and prey vulnerability, it is possible to compare the simulated course of the mean food selectivity (cf. Fig. 2e, f) with the observed course of the relative importance of filter and interception feeders (Fig. 5b). Both, the simulated food selectivity and the two observed functional groups, exhibited recurrent changes (at least twofold in the field, unlimited in the model), albeit at different time scales. In the model, the time scale depends on the exact parameterization, e.g., on the absolute growth rates. The latter are also influenced by external forcing not included in the model. The different model species can be related to distinct algal and ciliate species dominating in Lake Constance during spring. For example, the less edible prey A_1 reflects the ecological characteristics of small diatoms, such as *Stephanodiscus parvus*; the highly edible prey A_3 reflects the ecological characteristics of cryptomonads, e.g., *Rhodomonas* spp.; whereas the nonselective consumer C_1 exhibits the characteristics of filter feeders, such as, e.g., *Rimostrombidum lacustris*,

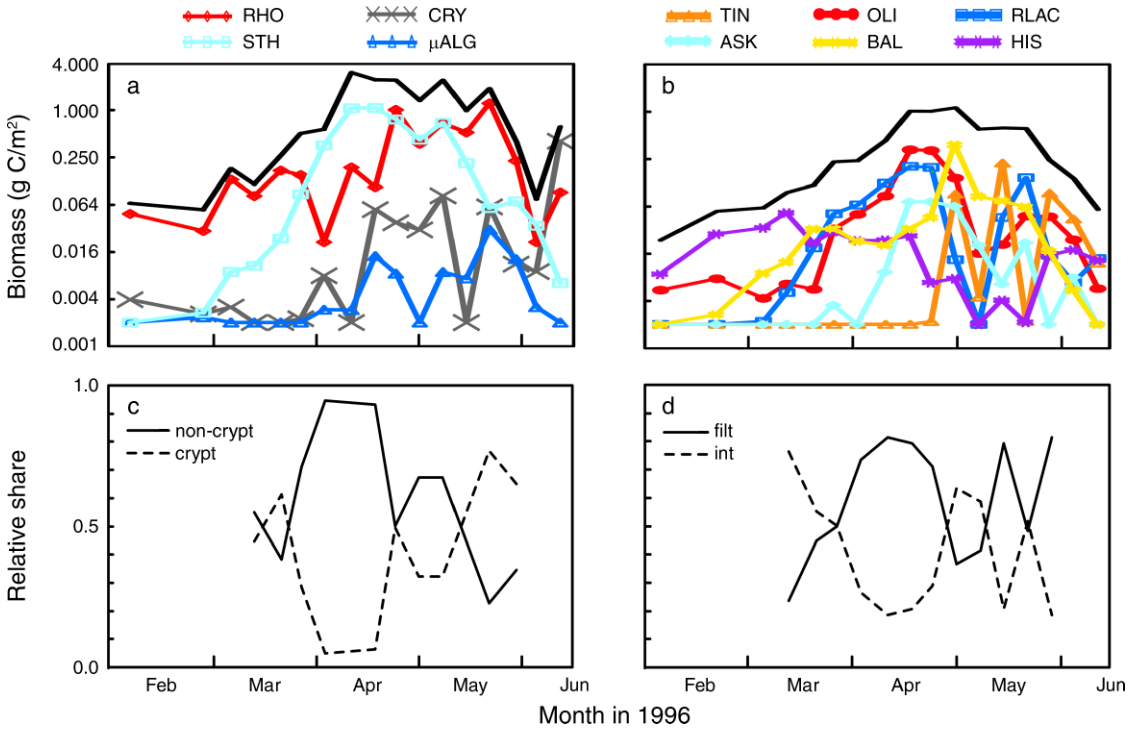

FIG. 5. Field data from Lake Constance during spring, February until mid-June in 1996 (= 136 d; figure redrawn from Tirok and Gaedke [2007]). (a, b) Biomass of the (a) prey (small edible algae) and the (b) predator community (algivorous ciliates) (black line = total biomass, colored lines = biomass of four exemplary algal and six exemplary ciliate species). (c, d) Relative share of two functional (c) algal and (d) ciliate groups in total biomass during the spring bloom (mid-March until end of May). Abbreviations are: crypt, cryptomonads (highly edible); non-crypt, non-cryptomonads (less edible); int, interception feeders (highly selective); filt, filter feeders (less selective); CRY, *Cryptomonas* spp.; μALG, small eukaryotic algae; RHO, *Rhodomonas* spp.; STH, *Stephanodiscus parvus*; TIN, tintinnids; OLI, oligotrichs <35 μm; RLAC, *Rimostrombidium lacustris*; ASK, *Askenasia* sp.; BAL, *Balanion planctonicum*; HIS, *Histobalantium bodamicum* (for more details, see Tirok and Gaedke [2007]).

and the selective consumer C_3 those of interception feeders, such as, e.g., *Balanion planctonicum*.

Our model approach uncovered a potential mechanism for how the observed cyclic changes in species abundances can be driven by an internal feedback mechanism, i.e., by the predator–prey interactions themselves. In the model, this internal feedback system results in an ongoing change of species composition (limit cycle), and in a coexistence at high biomass levels. In Lake Constance, such coexistence at a high biomass level is also maintained for about 10–30 generations until other forces, such as increasing predation by larger zooplankton on both the algae and their ciliated predators, terminate the spring bloom.

Generalization

In general, three conditions have to be fulfilled for the occurrence of such internal feedbacks: (1) interactions between two diverse trophic levels dominate over abiotic factors with (2) top-down control of the lower trophic level (prey) and bottom-up control of the higher trophic level (predators), and (3) both 1 and 2 prevail for a prolonged time period (many generations). That is, such dynamics may develop in any functional diverse predator–prey system. The dynamics produced by the multispecies model was not sensitive to changes in the growth rate of the prey (changes in $b_{r'}$ or K) or the predator (changes in b_M, g', e, or d) which may arise from seasonal and stochastic variation, e.g., in temperature and light. Furthermore, our model was independent of the initial conditions, i.e., it returned to the same dynamics after being disturbed. The internal dynamics may be disrupted when the top-down control by the higher trophic level breaks down, either due to abiotic forces, e.g., dilution of the populations due to intense vertical mixing in deep waters, or due to biotic forces, e.g., strong predation on the upper trophic level. This may occur in real ecosystems, since such individual predator–prey systems as assumed in this model study are typically embedded into a larger food web. Thus, they are influenced by and may in turn affect other members of the food web and food web dynamics. The dynamics of our food web did not depend on the symmetry of its setup. We did not consider several distinct "predator–prey pairs," but one predator feeding on all prey species (nonselective) and thus strongly linking all members of the food web, and one predator feeding preferentially on one prey species forming a predator–prey pair. As long as such functionally different predators existed, they exhibited compensatory

dynamics as did the intermediate species unless it was functionally rather similar to one of the others. The latter promoted synchronization between the two species but not with the third one. That is, our model was less sensitive to the specific geometry of parameterization and functional differences than, e.g., a one-trophic-level competition model by Huisman and Weissing (2001) leading to coexistence of many (plant) species relying on few resources driven by species oscillations. What is required in our model is the occurrence of at least one selective predator. Here, we restricted our considerations to three functionally different predator and prey species. In addition to the functional diversity, the number of species may play a role, a topic that is being investigated currently (B. Bauer, M. Vos, and U. Gaedke, *unpublished manuscript*).

Species alternations

The cyclic change in the abundance of different species results in an ongoing balancing and maintenance of trophic level integrity. If one species is no longer "optimally" tuned to the prevailing conditions, the species, which is better suited for those conditions gains in importance as long as it is doing better than the others. Conditions can change externally due to environmental fluctuations, but also internally by the species interactions themselves as done in the present predator–prey system. For a certain composition of the prey community there can be one best suited predator species. However, if this species increases, the conditions in terms of the grazing impact change for the prey community, and thus its species composition will shift which in turn implies an altered food availability for the (prevailing) predator. This mechanism functions as long as trade-offs exist, that is, an advantage in one trait is connected to a disadvantage in another trait, and the individual fitness of a species depends on which trait is in demand at a given moment which continuously changes due to the feedback to the predator. The cyclic changes in species abundances did not fade out for more then 10^7 time steps and were not restricted to a high carrying capacity. Considering these inevitable and ubiquitous trade-offs among the different physiological and ecological characteristics of the individual species in the model prevented an ongoing dominance or the extinction of particular functional types for a wide parameter space. The model behavior was not sensitive to the exact specification of the trade-off functions.

Remarkably, this effect even allowed that the prey spectrum of the selective consumer was entirely included in that of the intermediate, and of the nonselective consumer. Given such a food web structure, coexistence is not mandatory as the nonselective predator may depress the prey of the selective one to very low levels by feeding on its additional prey which was the case when no trade-offs existed (cf. scenario 0, Figs. 3, 4a). Coexistence of selective and nonselective consumers was related to the lower food quantity demand of the selective consumer, and from the typically high productivity of the highly edible prey species that is eaten by many predators. Thereby, the selective consumer achieved positive net population growth during peaks of its preferred prey, whereas the nonselective consumer relied on the mean value of the entire prey community.

In an experimental and modeled predator–prey system, the genetic diversity of the prey was manipulated (Yoshida et al. 2003, 2007). Low diversity produced short cycles and typical quarter-period phase lags between prey and predator densities, whereas a genetically variable prey population produced long cycles with prey and predator nearly out of phase. This could even result in so called "cryptic predator–prey cycles" as the strong coupling between predator and prey became not obvious (Yoshida et al. 2007). This was attributed to adaptation of the prey community, which shifted to lower edibility when the grazing pressure was high. In our model, allowing for functional change at both the prey and the predator level, the typical predator–prey cycles disappear as well.

Compensatory dynamics

Temporal variability decreases from the population to the community level depending on the diversity and the degree of synchronization among dominant populations (Hooper et al. 2005). In our model, the trade-offs specified the degree of functional diversity and determined whether compensatory or synchronous dynamics occurred, and consequently how strong total plant and herbivore biomass may be stabilized. Compensatory dynamics are typically attributed to differential responses to abiotic forcing (Ives et al. 1999, Hooper et al. 2005). In contrast, our model, which did not include any external forcing, exemplifies that compensatory dynamics and synchronization may also arise from internal mechanisms, and that compensatory and synchronous dynamics may alternate in time within the same system.

Compensatory dynamics were promoted in particular at high prey biomass by the joint carrying capacity linking the three prey species and the identical capabilities of all prey species to use the shared resources (cf. Eq. 3; Vandermeer 2004, 2006), since under these conditions a biomass decrease of one prey species promoted the growth of the other ones. In contrast, synchronization is enhanced by the coupling of the different predator and prey species via common feeding links (Vandermeer 2006). For example, a high biomass and thus grazing pressure of a nonselective predator tends to directly synchronize the prey species and to reduce the impact of the joint carrying capacity, promoting compensatory dynamics when algal biomasses are low. Furthermore, choosing more similar values of the feeding preferences led to ecologically more similar species and stronger interactions and increased the degree of synchronization of the individual prey and predator species. As the functionally different species alternated in their relative importance and absolute

biomasses varied during parts of each time series, the strength of the mechanisms promoting synchronization and compensatory dynamics were highly variable in time. This yielded complex dynamical patterns with species being partly in or out of phase and a temporally variable degree of damping (e.g., Fig. 4b). Such a temporal alternation of compensatory and synchronous dynamics within one system was observed between edible and less-edible phytoplankton species in Lake Constance (Vasseur et al. 2005). Most species were synchronized during winter (low biomasses) and spring (biomass increasing) due to overall adverse and subsequently improving growth conditions, and out of phase during summer due to differential grazing pressure.

We observed consistent compensatory dynamics only for intermediately strong trade-offs in both the prey and the predator community. That is, both communities had to be functionally diverse to yield such compensation. In contrast, when predator species were rather similar they tended to cycle more synchronously, resulting in synchronization of the prey species. This effect was slightly decreased with increasing differences between the prey species. For exceedingly different species, typically one became superior and outcompete the others, thus preventing substantial compensation.

Conclusions

Our model analysis considered the effects of general trade-offs and functional diversity in multispecies predator–prey communities. We identified conditions when the dynamics of such communities result in internally driven alternations of functional traits, coexistence and compensation, and contrast this with scenarios that lead to synchronization and competitive exclusion. Our findings deliver a consistent explanation for complex dynamics observed in the field and they have wider implications beyond the predator–prey system studied here, as adaptation processes such as those considered here are very likely to occur in numerous other systems and at other hierarchical levels (e.g., shifts in genotypes). Future work should establish to what extent qualitatively different trade-offs than those studied here would affect the likelihood of compensatory dynamics and community level damping of biomasses. This study shows that the degree of functional diversity may strongly influence the variability of ecosystem functions, as it affects the dynamical behavior, species coexistence, and the absolute level of temporal variability and its damping at a higher hierarchical level.

Acknowledgments

This work was strongly inspired by discussions with Kai Wirtz. We gratefully acknowledge Matthijs Vos for interesting and constructive discussions and for improving the manuscript. We also thank Barbara Bauer for constructive discussions, Wolfgang Ebenhöh for helpful comments on the model equations and sensitivity analysis, and Sebastian Diehl, Gregor Fussmann, and Guntram Weithoff for critical reading of an earlier version of the manuscript. K. Tirok was funded by the German Research Foundation (DFG) within the Priority Program 1162 "The impact of climate variability on aquatic ecosystems (AQUASHIFT)" (GA 401/7-1).

Literature Cited

Baretta-Bekker, J. G., J. W. Baretta, A. S. Hansen, and B. Riemann. 1998. An improved model of carbon and nutrient dynamics in the microbial food web in marine enclosures. Aquatic Microbial Ecology 14:91–108.

Baretta-Bekker, J. G., J. W. Baretta, and E. K. Rasmussen. 1995. The microbial food-web in the European-Regional-Seas-Ecosystem-Model. Netherlands Journal of Sea Research 33:363–379.

Elton, C., and M. Nicholson. 1942. The ten-year cycle in numbers of the lynx in Canada. Journal of Animal Ecology 11:215–244.

Fenchel, T. 1987. Ecology of protozoa: the biology of free-living phagotrophic protists. Brock/Springer Series in Contemporary Bioscience, Science Tech Publishers, Madison, Wisconsin, USA.

Fussmann, G., S. Ellner, K. Shertzer, and N. Hairston. 2000. Crossing the Hopf bifurcation in a live predator–prey system. Science 290:1358–1360.

Gaedke, U., S. Hochstädter, and D. Straile. 2002. Interplay between energy limitation and nutritional deficiency: empirical data and food web models. Ecological Monographs 72: 251–270.

Grime, J. 1977. Evidence for existence of 3 primary strategies in plants and its relevance to ecological and evolutionary theory. American Naturalist 111:1169–1194.

Hamels, I., H. Mussche, K. Sabbe, K. Muylaert, and W. Vyverman. 2004. Evidence for constant and highly specific active food selection by benthic ciliates in mixed diatoms assemblages. Limnology and Oceanography 49:58–68.

Hooper, D., et al. 2005. Effects of biodiversity on ecosystem functioning: a consensus of current knowledge. Ecological Monographs 75:3–35.

Huisman, J., A. Johansson, E. Folmer, and F. Weissing. 2001. Towards a solution of the plankton paradox: the importance of physiology and life history. Ecology Letters 4:408–411.

Huisman, J., and F. Weissing. 2001. Fundamental unpredictability in multispecies competition. American Naturalist 157: 488–494.

Ives, A. R., K. Gross, and J. L. Klug. 1999. Stability and variability in competitive communities. Science 286:542–544.

Kümmerlin, R. 1991. Long term development of phytoplankton in Lake Constance. Verhandlungen der Internationalen Vereinigung für Limnologie 24:826–830.

Litchman, E., and C. A. Klausmeier. 2008. Trait-based community ecology of phytoplankton. Annual Review of Ecology, Evolution, and Systematics 39:615–639.

Litchman, E., C. Klausmeier, O. Schofield, and P. Falkowski. 2007. The role of functional traits and trade-offs in structuring phytoplankton communities: scaling from cellular to ecosystem level. Ecology Letters 10:1170–1181.

Lotka, A. 1925. Elements of physical biology. William and Wilkins, Baltimore, Maryland, USA.

Luckinbill, L. 1979. The effects of space and enrichment on a predator–prey system. Ecology 55:1142–1147.

McCann, K. 2000. The diversity-stability debate. Nature 405: 228–233.

McCauley, E., R. Nisbet, W. Murdoch, A. de Roos, and W. Gurney. 1999. Large-amplitude cycles of *Daphnia* and its algal prey in enriched environments. Nature 402:653–656.

McGill, B., B. Enquist, E. Weiher, and M. Westoby. 2006. Rebuilding community ecology from functional traits. Trends in Ecology and Evolution 21:178–185.

Müller, H. 1989. The relative importance of different ciliate taxa in the pelagic food web of Lake Constance. Microbial Ecology 18:261–273.

Müller, H., and A. Schlegel. 1999. Responses of three freshwater planktonic ciliates with different feeding modes to cryptophyte and diatom prey. Aquatic Microbial Ecology 17:49–60.

Müller, H., A. Schöne, R. Pinto-Coelho, A. Schweizer, and T. Weisse. 1991. Seasonal succession of ciliates in Lake Constance. Microbial Ecology 21:119–138.

Norberg, J. 2004. Biodiversity and ecosystem functioning: a complex adaptive systems approach. Limnology and Oceanography 49:1269–1277.

Reynolds, C. 1997. Vegetation processes in the pelagic: a model for ecosystem theory. Ecology Institute, Oldendorf/Luhe, Germany.

Rosenzweig, M., and R. MacArthur. 1963. Graphical representation and stability conditions of predator–prey interactions. American Naturalist 97:209–223.

Rothhaupt, K. 1990. Resource competition of herbivorous zooplankton: a review of approaches and perspectives. Archiv für Hydrobiologie 118:1–29.

SAS Institute. 2002. SAS version 9.0. SAS Institute, Heidelberg, Germany.

Schluter, D. 1984. A variance test for detecting species associations, with some example applications. Ecology 65: 998–1005.

Skogstad, A., L. Granskog, and D. Klaveness. 1987. Growth of fresh-water ciliates offered planktonic algae as food. Journal of Plankton Research 9:503–512.

Sommer, U., U. Gaedke, and A. Schweizer. 1993. The 1st decade of oligotrophication of Lake Constance. 2. The response of phytoplankton taxonomic composition. Oecologia 93:276–284.

Sommer, U., Z. Gliwicz, W. Lampert, and A. Duncan. 1986. The PEG-model of seasonal succession of planktonic events in fresh waters. Archiv für Hydrobiologie 106:433–471.

Sommer, U., F. Sommer, B. Santer, E. Zöllner, K. Jürgens, C. Jamieson, M. Boersma, and K. Gocke. 2003. *Daphnia* versus copepod impact on summer phytoplankton: functional compensation at both trophic levels. Oecologia 135:639–647.

Stearns, S. 1992. The evolution of life histories. Oxford University Press, New York, New York, USA.

Thebault, E., and M. Loreau. 2005. Trophic interactions and the relationship between species diversity and ecosystem stability. American Naturalist 166:E95–E114.

Thebault, E., and M. Loreau. 2006. The relationship between biodiversity and ecosystem functioning in food webs. Ecological Research 21:17–25.

Tilman, D., S. S. Kilham, and P. Kilham. 1982. Phytoplankton community ecology: the role of limiting nutrients. Annual Review of Ecology and Systematics 13:349–372.

Tirok, K., and U. Gaedke. 2007. Regulation of planktonic ciliate dynamics and functional composition during spring in Lake Constance. Aquatic Microbial Ecology 49:87–100.

Vandermeer, J. 2004. Coupled oscillations in food webs: balancing competition and mutualism in simple ecological models. American Naturalist 163:857–867.

Vandermeer, J. 2006. Oscillating populations and biodiversity maintenance. BioScience 56:967–975.

Vasseur, D., U. Gaedke, and K. McCann. 2005. A seasonal alternation of coherent and compensatory dynamics occurs in phytoplankton. Oikos 110:507–514.

Verity, P. 1991. Feeding in planktonic protozoans: evidence for nonrandom acquisition of prey. Journal of Protozoology 38: 69–76.

Vinebrooke, R., D. Schindler, D. Findlay, M. Turner, M. Paterson, and K. Milis. 2003. Trophic dependence of ecosystem resistance and species compensation in experimentally acidified lake 302S (Canada). Ecosystems 6:101–113.

Volterra, V. 1926. Fluctuations in the abundance of a species considered mathematically. Nature 188:558–560.

Weisse, T., and H. Müller. 1998. Planktonic protozoa and the microbial food web in Lake Constance. Archiv für Hydrobiologie Special Issue. Advances in Limnology 53:223–254.

Weithoff, G. 2003. The concepts of "plant functional types" and "functional diversity" in lake phytoplankton: a new understanding of phytoplankton ecology? Freshwater Biology 48:1669–1675.

Wirtz, K., and B. Eckhardt. 1996. Effective variables in ecosystem models with an application to phytoplankton succession. Ecological Modelling 92:33–53.

Yoshida, T., S. P. Ellner, L. E. Jones, B. J. M. Bohannan, R. E. Lenski, and N. G. Hairston, Jr. 2007. Cryptic population dynamics: rapid evolution masks trophic interactions. PLoS Biology 5:1868–1879.

Yoshida, T., N. Hairston, and S. Ellner. 2004. Evolutionary trade-off between defence against grazing and competitive ability in a simple unicellular alga, *Chlorella vulgaris*. Proceedings of the Royal Society B 271:1947–1953.

Yoshida, T., L. Jones, S. Ellner, G. Fussmann, and N. Hairston. 2003. Rapid evolution drives ecological dynamics in a predator–prey system. Nature 424:303–306.